HHS Public Access

Author manuscript

Epilepsy Res. Author manuscript; available in PMC 2021 January 01.

Published in final edited form as:

Epilepsy Res. 2020 January ; 159: 106255. doi:10.1016/j.eplepsyres.2019.106255.

Emerging roles of network analysis for epilepsy

William Stacey[1,*], **Mark Kramer**[2], **Kristin Gunnarsdottir**[3], **Jorge Gonzalez-Martinez**[4], **Kareem Zaghloul**[5], **Sara Inati**[6], **Sridevi Sarma**[3], **Jennifer Stiso**[7], **Ankit N. Khambhati**[7], **Danielle S. Bassett**[7], **Rachel J. Smith**[8], **Virginia B. Liu**[9,10], **Beth A. Lopour**[8], **Richard Staba**[11]

[1]Department of Neurology, Department of Biomedical Engineering, University of Michigan

[2]Department of Mathematics and Statistics, Center of Systems Neuroscience, Boston University

[3]Department of Biomedical Engineering, Johns Hopkins University

[4]Department of Neurological Surgery, University of Pittsburgh

[5]Surgical Neurology Branch, National Institute of Neurological Disorders and Stroke, NIH

[6]Office of the Clinical Director, National Institute of Neurological Disorders and Stroke, NIH

[7]Department of Bioengineering, University of Pennsylvania

[8]Department of Biomedical Engineering, University of California, Irvine

[9]Department of Pediatrics, University of California, Irvine

[10]Department of Child Neurology, Children's Hospital of Orange County, California

[11]Department of Neurology, David Geffen School of Medicine at UCLA, Los Angeles, CA

Abstract

In recent years there has been increasing interest in applying network science tools to EEG data. At the 2018 American Epilepsy Society conference in New Orleans, LA, the yearly session of the Engineering and Neurostimulation Special Interest Group focused on emerging, translational technologies to analyze seizure networks. Each speaker demonstrated practical examples of how network tools can be utilized in clinical care and provide additional data to help care for patients with intractable epilepsy. The groups presented advances using tools from functional connectivity, control theory, and graph theory to analyze human EEG data. These tools have great potential to augment clinical interpretation of EEG signals.

Keywords

EEG; Network analysis; Functional Connectivity; Graph Theory; Control Theory; Infantile Spasms

[*]Corresponding author: William.stacey@umich.edu, 1500 E. Medical Center Drive SPC 5036, Ann Arbor, MI 48109.

1.1 Introduction

For the past two decades, there has been steadily increasing interest in applying engineering tools to epilepsy care (Stacey and Litt, 2008). These tools encompass both analysis and treatment, and span a broad range of techniques. The earliest tools were quantitative EEG analysis, e.g. automated spike and seizure detectors, and electrical stimulation. Both aspects have achieved commercial and clinical success recently, but there is still much room for improvement. The American Epilepsy Society organized two Special Interest Groups that encompassed these two specialties: Engineering in Epilepsy and Neurostimulation. These two were combined several years ago into the current Engineering/Neurostimulation Group, which has dedicated sessions at every annual meeting of the American Epilepsy Society. This work details the proceedings for the meeting in December 2018 in New Orleans, which focused on tools for network analysis of EEG.

EEG signals are ideal for a host of signal processing tools. Yet clinical implementation of such tools has been very slow. In a review article in 1975, pioneering EEG engineer Harold Shipton noted that visual interpretation of EEG "has remained the method of choice…while the tools of information engineering, mathematical and statistical analysis, and computer science are little used and less respected…New instrumental methods can be expected to displace the eyeball as an analytic tool [via] the long-awaited and often-announced marriage between EEGer and computer scientist" (Shipton, 1975). Those words, written over 40 years ago, are still pertinent today. There have been some significant advancements: commercial software now allows direct visualization of quantitative EEG within the clinical viewer, and several clinically-approved devices are now implanted to control intractable epilepsy with electrical stimulation. Yet all of these products use methods that are only slight modifications of the tools available to Shipton in 1975. One aspect of "mathematical and statistical analysis" that was not available in 1975 is network analysis, which has grown tremendously in recent years and is especially applicable to epilepsy research. In the 2018 session of the Engineering/Neurostimulation meeting, four research groups presented the current state-of-the-art for network analysis in epilepsy, each with a specific goal of presenting results designed for clinical use. The first session presented a primer on network analysis and introduced a freely-downloadable pipeline that can be integrated with various different types of network tools. This was followed by three groups using distinct network analysis methods to interpret human EEG data.

2.1 An Introduction to Network Analysis & EEG Interpretation

Network analysis is in the midst of extreme growth, both in the development of new tools and in the adoption in various fields. Neuroscience is a natural fit for such analyses, as there are vast quantities of data acquired across large spatial and temporal scales. While a full review of these techniques is beyond the scope of this article, the reader is invited to several comprehensive reviews on the subject (Bassett and Sporns, 2017; Bassett et al., 2018; Stefan and Lopes da Silva, 2013; van Diessen et al., 2013). One of the basic tenets of connectivity analysis is the concept of nodes and edges. In neuroscience, a node typically represents a region of homogeneous activity. In the case of EEG data, a node is often the location of the recording electrode, or a region of brain activity estimated from the EEG data (e.g. source

estimation (Gramfort et al., 2014)). An edge is a theoretical connection between different nodes, which can take a wide variety of physiological meanings. When an edge quantifies the functional connectivity between two nodes, the edge indicates similar activities occur at the two nodes. There are many different methods to define and measure such similarities of activity. Given the wide range of tools found in the literature, in this first section we briefly introduce an example of functional connectivity analysis as applied to study human seizures. We propose a functional network analysis pipeline (Figure 1), and describe the decisions associated with implementing this pipeline in practice. We provide an example data set and code so that the interested reader may explore an instance of this functional network analysis pipeline.

For concreteness, we focus on functional connectivity between multivariate brain voltage signals (e.g., recordings from the scalp EEG). The goal of functional network analysis is to understand which signals are coupled and when this coupling occurs. While the analysis of coupling between brain voltage signals in patients with epilepsy has a long history (Brazier, 1972; Gotman, 1983), the application of network analysis is relatively new. Here we propose a five-step procedure to apply functional network analysis in practice; we briefly describe below the decisions and challenges associated with each step.

1. Data collection: Recordings typically trade off spatial sampling for brain coverage. For example, while microelectrode array recordings provide excellent spatial resolution (< 1mm), the brain coverage is poor (e.g., isolated to one small patch of cortex). Alternatively, scalp EEG provides excellent brain coverage, with poor spatial sampling (on the order of 10 cm^2 of cortex). The choice of data collection method determines the number of nodes in the network (e.g., high density EEG provides more nodes than low density EEG), and the rhythms observable (e.g., high temporal sampling supports analysis of coupling between faster brain rhythms).

2. Re-referencing: EEG is typically recorded by referencing all the recording channels to a defined reference electrode, which differs in different laboratories. These single channels are then re-referenced for better viewing. Many schemes exist to reference brain voltage signals, and no reference choice is optimal in all recording scenarios. Common re-referencing schemes include bipolar, common average, Laplacian, and more computationally advanced techniques (Yao, 2001). Each choice impacts the functional network features inferred. For example, a bipolar montage reduces the number of nodes in the network, while a common average reference introduces a shared signal between all sensors. The reference choice should be carefully considered when interpreting functional network analysis results.

3. Filtering: EEG data are filtered to isolate specific frequency bands for analysis, and remove artifacts from the data (e.g., sweat artifact, 60 Hz line noise). Filtering requires the selection of many parameters (e.g., the filter type, order, attenuation), which again may impact the networks inferred. For example, narrowband filtering may introduce artifactual coupling between sensors, or obfuscate coupling in alternative frequency bands. For example, two unrelated

time series—each filtered to 4–6 Hz—may appear coupled during short intervals of time (e.g. within 1 sec intervals). Conversely, focusing on a narrow band ignores coupling outside this band.

4. Network inference: Many measures exist to assess coupling between time series (Greenblatt et al., 2012; Pereda et al., 2005), each with advantages and disadvantages. This step essentially defines and measures the edges within the network analysis framework. Measures of linear coupling (e.g., cross-correlation) are simple, fast to compute, and possess well understood statistical properties. Measures of nonlinear coupling (e.g., information) more accurately identify subtle interactions, but are more complex – both to understand and assess. Model based measures of coupling (e.g., Granger causality) address important confounds in existing measures, but are computationally intractable for networks with many nodes (although new procedures help overcome this limitation (Spencer et al., 2018)). The resulting networks may include edges weighted by the strength of the coupling measure, or binary networks with edge threshold defined by the strength of the coupling measure or its level of significance.

5. Network analysis: Many measures exist to analyze the spatiotemporal properties of a network inferred in Step 4. These include static measures (e.g., path length, clustering coefficient, modularity) (Rubinov and Sporns, 2010) and newly emerging dynamic measures (e.g., measures of how community organization evolves in time) (Bassett and Sporns, 2017).

We note that the five steps in the proposed functional network analysis pipeline are interconnected. For example, choosing a common average reference (Step 2) impacts the network results (Step 5); choosing a network inference method (e.g., coherence in a specific frequency band in Step 4) impacts the filtering choice (Step 3).

The interested reader is encouraged to access the repository https://github.com/Mark-Kramer/AES-SIG-2018 for an example application of the proposed functional network analysis pipeline. In this example, we make a specific choice for each step. However, we note that not every choice is a good one, and emphasize that the example serves only as a guide, not a solution.

Epilepsy is considered a network disease, with network features that span from the microscopic scale of single neurons to the macroscopic scale of the entire central nervous system. While intuitively appealing, how to apply this network concept in clinical practice remains unclear. A consistent functional network analysis pipeline would enhance the rigor and reproducibility of network results, and perhaps improve clinical application of network features to patients with epilepsy.

3.1 Using Network Models of Invasive EEG to Solve the Missing Electrode Problem

Clinical decisions in refractory epilepsy depend upon correct identification of the epileptogenic zone (EZ), which is defined as the minimal area of brain tissue responsible for generating the recurrent seizure activity (Luders et al., 2006). However, the EZ is a theoretical designation as there is no gold standard to identify it. As proof that standard clinical procedures do not always correctly identify the EZ, seizure freedom rates after surgical resection vary between 30 and 70% (Bulacio et al., 2012; Gonzalez-Martinez et al., 2007).

Surgical treatment can fail to control or eliminate drug-resistant seizures for a number of reasons. One clear limitation is that the clinical decision is based upon interpretation of the EEG. Intractable seizures often require implanted electrodes to improve localization of the EZ. These include subdural electrodes (i.e. grids or ECoG) and depth electrodes, which are becoming increasingly popular using stereo-EEG (SEEG). However, both types have a clear undersampling problem, and clinical interpretation of the data is often limited. Physiologically, there are additional confounding factors that can lead to surgical failure. For instance, some patients have an epileptogenic lesion or multiple lesions that involve both hemispheres and surgical resection cannot remove all of the lesion. In other cases, the brain areas to be resected involve motor, speech, or visual cortex and cannot be completely removed without creating significant functional deficits. Thus, even with the best available technology, our understanding of how to define and treat the EZ is still limited.

Modern state-of-the-art involves a surgical implantation of subdural or depth electrodes followed by a visual inspection of hundreds of corresponding EEG signals before and during seizure events that occur over several days to weeks. Clearly, surgical outcome relies heavily on precise placement of electrodes such that they cover the hypothetical EZ. Ideally, one would like a highly dense coverage of brain regions to obtain clear boundaries of the EZ. Unfortunately, this is not possible due to surgical limitations associated with massive implantation of hundreds of electrodes. This gives rise to the *"missing electrode problem,"* where clinicians desire to know what neural activity looks like near and between implanted electrodes.

The goal of this project is to develop a computational tool that provides a denser brain coverage by estimating neural activity at "desired" missing electrode locations from measured signals in focal medically-refractory epilepsy (MRE) patients undergoing invasive monitoring. To achieve this goal we will perform the following processing steps: (i) process diffusion tensor imaging (DTI) data to identify structural (anatomical) connectivity patterns between all brain regions; (ii) process fMRI and MEG recordings to obtain functional dependencies between all brain regions; (iii) derive a dynamical network model of brain activity, by integrating structural connectivity and functional dependencies of the whole brain with functional information available from ECoG or SEEG data; and finally (iv) use an observer (from control theory) in conjunction with the dynamical network model of the brain to estimate ECoG or SEEG activity of clinically determined missing electrodes.

3.2 Estimating Patient-Specific Network Models

To accomplish those four processing steps, in this paper we develop and test a computational tool that constructs dynamical network EEG models from noninvasive structural (DTI) and functional imaging (fMRI, MEG) data, and functional invasive EEG (ECoG and SEEG) data. Specifically, we will compute linear time invariant (LTI) network models in 500 msec windows, where $\boldsymbol{x}(t)$ is called the state vector and represents the activity on all the electrodes, and $\boldsymbol{A}$ is the state transition matrix that defines how the electrodes interact and how the activity evolves over time. Further definition of the state and the network model is shown in Fig. 2 A,B. Note that $\boldsymbol{x}(t)$ represents both implanted and missing electrodes, and is partitioned into the measured, $\boldsymbol{x}^m(t)$, and unmeasured ("missing'") states, $\boldsymbol{x}^u(t)$. Although EEG recordings are not generated from an LTI network in practice, we have shown in our previous work that in very small windows (e.g. 500 msec), an LTI model can be estimated to accurately reconstruct the data (Li et al., 2017). Thus, the entire EEG window can be represented as a linear time *varying* network where the $\boldsymbol{A}$ matrix changes in each 500 msec window (Li et al., 2017). If we had access to all signals, we could simply estimate the sequence of $\boldsymbol{A}$ matrices. However, since we only have access to the measured signals, we can estimate the smaller block matrix in each $\boldsymbol{A}$, denoted as $\boldsymbol{A}_{mm}$ in Fig. 2B, from the observed signals, and the rest of the $\boldsymbol{A}$ matrix ($\boldsymbol{A}_{mu}, \boldsymbol{A}_{um}, \boldsymbol{A}_{uu}$), i.e. the unmeasured signals, must be estimated from noninvasive imaging data (DTI, fMRI, and MEG).

Specifically, we will construct connectivity matrices from DTI data by computing structural connectivity between regions corresponding to the EEG (ECoG or SEEG) electrodes *and* specified missing electrodes. We will also construct functional connectivity matrices (e.g. correlation matrices) from both fMRI and MEG recordings for the implanted electrode regions *and* missing electrode regions. Matrices constructed from these noninvasive modalities will be used to initialize ($\boldsymbol{A}_{mu}, \boldsymbol{A}_{um}, \boldsymbol{A}_{uu}$) for each 500 msec window, which are not identifiable from the measured EEG signals. Finally, these models will be used to estimate missing electrode signals using "observers" from control theory. See Fig. 2C.

3.3 Reduced-Order Observer

We will implement an observer from control theory to reconstruct the missing signals ($\boldsymbol{x}^u(t)$) from the measured signals ($\boldsymbol{x}^m(t)$). An observer (Luenberger, 1964) is an algorithm that provides an estimate of the *entire* internal state vector of a system (e.g. the epileptic brain network) using the system's model parameters ($\boldsymbol{A}$) and measurements of the system's output (measured EEG signals). Observers are familiar to control theorists, and in this case provide an intriguing tool to solve the missing electrode problem for clinicians (Gunnarsdottir et al., 2017).

To understand how observers work, let's consider an ecosystem with lions and gazelles (Fig. 2). Lions eat gazelles and gazelles eat grass. We can describe how the population of gazelles at some time t, $x_1(t)$, affects the population of lions, $x_2(t)$, with a predator-prey model. The nonlinear dynamical 2-node network model is provided in Fig. 2, which incorporates the birth and death rates of each species as well as their interactions. Now, suppose we could only observe the number of lions over time *and* we had access to the model. i.e., $\{a, b, c, d\}$,

then we could estimate the number of gazelles over time. Intuitively, this makes sense. For example, you observe that the population of lions is declining, then that means that they are starving and thus the number of gazelles is declining at that time. The algorithm that provides the estimate is an *observer*.

For our application, only a part of the state, $\boldsymbol{x}^u(t)$, is unknown, and thus we implemented an iterative approach using a reduced-order observer (Gunnarsdottir et al., 2017) to estimate only the signals at the missing contacts. Note that we only know $\boldsymbol{x}^m(t)$ in our application, but the observer requires that we also know the model parameters of the brain network ($\boldsymbol{A}$) in order to estimate the missing signals. Thus, we need to construct $\boldsymbol{A}$ and the estimate for $\boldsymbol{x}^u(t)$ (denoted $\hat{\boldsymbol{x}}^u(t)$) simultaneously for each 500 msec window in the EEG series, which we describe next.

3.4 Algorithm – estimating the network model and missing signals

This tool comprises an iterative algorithm that simultaneously generates (i) an estimate of the network model, $\widehat{\boldsymbol{A}}$, for each 500 msec window, as well as (ii) estimates of the signals from the "missing" electrodes, $\hat{\boldsymbol{x}}^u(t)$. Note that the estimated model, $\widehat{\boldsymbol{A}}$, for each 500 msec window characterizes dynamics for each EEG contact, including the "missing" electrode contacts.

The tool first selects an initial model, denoted as $\boldsymbol{A}_0$, and then applies the observer to estimate the missing signals. Then, the algorithm uses the new missing signal estimates along with the measured signals to re-estimate the model (Dempster et al., 1977). Next, the new model is used to obtain new estimates of the missing signals recursively until it meets a user-specified stopping criterion. We have shown that this algorithm reliably estimates the missing signals (Gunnarsdottir et al., 2019).

3.5 Estimation of initial network model

The tool constructs excellent estimates of missing electrode signals when the model $\boldsymbol{A}$ is known (Gunnarsdottir et al., 2019). However, in reality we do not know the model $\boldsymbol{A}$. We will take the following 4 step approach to initialize $\boldsymbol{A}$ for each 500 msec window.

1. We will compute different structural connectivity matrices, from DTI data that captures strength of physical connections between all relevant brain regions (implanted and missing regions) using MRICloud (Mori et al., 2016). Specifically, white matter fiber tractography will be performed and inter-regional connectivity will be computed by determining the relative proportion of extracted fibers initiated or terminated within the boundaries of each relevant anatomical parcel. Various fractional anisotropy (FA) or diffusivity metrics will be tested to construct different structural connectivity matrices (Soares et al., 2013).
2. We will compute functional connectivity matrices from fMRI and/or MEG data that capture correlations between all relevant brain regions (implanted and missing regions) using MATLAB. Pairwise linear correlations (e.g. Pearson),

coherence in a given frequency bands (Bowyer, 2016; Lachaux et al., 1999), and phase synchrony between pairs of signals (Lachaux et al., 1999) will be tested.

3. We will use least squares estimation to construct $\boldsymbol{A}_{mm}$ from $\boldsymbol{x}_m(t)$ as done in (Li et al., 2017).

4. Finally, we will combine structural and functional information to estimate the initial model $\boldsymbol{A}_0$. Specifically, the structural matrices obtained in (1) and the functional matrices obtained in (2) will be used to constrain our initial model estimates. The block in $\boldsymbol{A}_0$ that corresponds to the measured signals will be replaced with the $\boldsymbol{A}_{mm}$ matrix from step (3).

3.6 Preliminary Data

In our previous work, we tested whether we could employ simple linear time-varying models to characterize invasive SEEG and ECoG data (Gunnarsdottir et al., 2019; Gunnarsdottir et al., 2017; Li et al., 2017), and then we used a reduced-order observer to simulate SEEG signals of unmeasured, "missing" electrodes. Fig. 4 shows an example where we implemented the approach described above using ECoG recordings from one focal MRE patient. Specifically, we removed 4 signals from a depth electrode (near the hypothetical EZ) from the data set and treated them as unmeasured, "missing" signals. Then the algorithm was used to estimate the missing signals. Our preliminary results suggest that control theoretic techniques can be employed to successfully estimate activity at "missing" electrode locations. Interestingly, in the example shown in Fig. 4, the missing electrodes had epileptic spiking activity not observed in the remaining electrodes. Yet, the algorithm was able to recover spikes from measured activity that had no spikes. This is very relevant as such spiking activity is often generated within the EZ.

3.7 Conclusions and Future Work

We have described early results from a computational tool that will provide a denser brain coverage in focal MRE patients undergoing invasive monitoring by estimating neural activity at "desired" missing electrode locations from signals of implanted electrodes. The tool comprises an iterative algorithm that simultaneously estimates (i) brain network models and (ii) the "missing" invasive EEG signals. Similar to many iterative algorithms (Karlis and Xekalaki, 2003), the performance of the tool is highly dependent on the initial network parameter estimates. We have shown that the algorithm constructs very good estimates of missing signals when the network model is known, and reliably recovers important signal characteristics for EZ localization, such as epileptic spiking activity. However, in practice the network model parameters will not be available to initialize the algorithm. Thus, our next steps include constructing initial model estimates that optimize performance by integrating whole brain structural and functional dependencies from non-invasive data with functional information available from ECoG or SEEG data, as described above. Finally, future work includes applying the tool to estimate clinically specified "missing" signals in a large set of patients and evaluate its performance on data from patients with both successful and failed surgical outcomes.

4.1 Network Science Approaches to Neural Function in Epilepsy

An increasing volume of data is available to support mapping the complex brain networks that underlie neurological diseases such as epilepsy. A critical challenge in the development of interventional tools for epilepsy is that of distilling biological mechanisms from network phenotypes of disease processes. Large volumes of data show that islands of synchronized neural activity dispersed across the epileptic brain can change regularly over the course of seizure progression, and those changes may mark times of heightened seizure risk (Litt et al., 2001; Warren et al., 2010). Because important features of epilepsy emerge on a network level, the tools that we use to inform interventions would benefit from network level analysis.

Network science is an emerging discipline that draws from graph theory and dynamical systems theory to characterize the local, global, and dynamic features of complex networked systems (Butts, 2009). Under this framework, functional neural networks are often defined as a series of brain regions (nodes) with statistical dependencies between region pairs (edges; Fig 5A). In an analogous mapping, structural neural networks are defined as a series of brain regions (nodes) with diffusion weighted imaging (DWI) estimates of white matter connections between region pairs (edges; Fig 5D). From such representations, we can examine the organizational principles of a network's connections at global or local scales. Global measures can quantify the *strength*, or sum of the connectivity of one region to every other region. In contrast, local measures can quantify the *pattern* of edges across all other regions. The paradigm of network neuroscience is already driving exciting work across many domains of inquiry including epilepsy (Jiruska et al., 2013; Khambhati et al., 2017). However, there is a fundamental gap in understanding how treatments for epilepsy, such as direct electrical stimulation, reliably alter network-level features and control seizures.

In a recent study, Khambhati et al. (Khambhati et al., 2019) sought to address this gap by characterizing how functional networks predictably change with stimulation. The authors used data from a cohort of 94 patients undergoing intracranial EEG monitoring for medically refractory epilepsy who also participated in an extensive stimulation regimen. They construct graph models in which intracranial sensors are represented by nodes and estimates of multitaper coherence between intracranial sensors are represented as edges for baseline, pre-stimulation, and post-stimulation epochs for each individual (Fig. 5A). They then evaluated how local and global measures changed between pre- and post-stimulation, and how these changes were mediated by baseline functional connectivity.

First, the authors hypothesized that stimulation can regularly elicit global changes in node strength, as well as local changes in the pattern of edges across the network. They found that in low frequencies (5–15 Hz), the magnitude of node strength regularly increases between pre- and post-stimulation epochs (Fig. 5B). Additionally, the magnitude of increase is correlated with baseline coherence with the stimulation site, indicating that baseline functional relationships constrain the network's response to stimulation (Fig. 5B). In contrast, local changes in the network's pattern of edges occurred strictly in high frequencies (95–105 Hz) (Fig. 5C). This effect shows a frequency dependent response, where a high stimulation frequency leads to larger changes in edge similarity (Fig. 5C).

Using 14 individuals in the stimulation cohort with diffusion weighted imaging of white matter architecture, the authors next asked how the pattern of structural connections from the stimulation site changed the network reconfiguration resulting from stimulation (Fig. 5D). Theoretical work in network control theory suggested ways in which the pattern of white matter connections could facilitate different strategies for changing activity of the network. One strategy, typically effective for areas with structurally weak connections, is to control small dynamic modes of a system, and thus effectively drive heterogeneous changes after stimulation (Feldt Muldoon et al., 2013; Pasqualetti et al., 2014). How well a region could enact this strategy is quantified by a metric called *modal controllability*. The authors hypothesized that stimulation to regions with high modal controllability would therefore result in spatially constrained effects, and lower overall functional reconfiguration. They found that in higher frequencies (15–25 Hz, 30–40 Hz, and 95–105 Hz), the modal controllability of the stimulated region was correlated with the average change in functional reconfiguration, such that stimulating stronger modal controllers led to smaller changes (Fig. 5E).

In summary, using intracranial recordings from patients with drug-resistant epilepsy, the authors test hypothesized rules that predict altered patterns of functional connectivity. They demonstrate that these functional interactions change in reliable ways based on stimulation frequency and location. These findings can now inform future research on optimizing and personalizing stimulation to modulate local and global properties of the epileptic network to make seizure control safer and more effective.

5.1 EEG-based functional connectivity networks as a marker of infantile spasms

Measurement of EEG-based functional connectivity networks (FCNs) can provide an objective characterization of underlying pathological brain activity associated with epilepsy. For example, abnormal FCNs derived from interictal EEG data are associated with temporal lobe epilepsy (Quraan et al., 2013), benign epilepsy with centrotemporal spikes (Adebimpe et al., 2016; Clemens et al., 2016), and generalized pharmacoresistant epilepsies (Horstmann et al., 2010). Recent evidence suggests that this is also true for infantile spasms, a pediatric epileptic encephalopathy characterized by clusters of seizures termed epileptic spasms (Hrachovy and Frost, 2003). Both EEG (Burroughs et al., 2014; Japaridze et al., 2013) and fMRI (Siniatchkin et al., 2007) studies have highlighted the role of cortical neuronal networks in infantile spasms, suggesting that EEG-based FCNs are a logical candidate from which to derive an objective marker of the disease.

FCNs can quantify clinically relevant characteristics of brain function that cannot be visually assessed, which is particularly valuable for infantile spasms. The EEG patterns classically associated with spasms, such as hypsarrhythmia, have a variable presentation (Hrachovy et al., 1984), leading to low interrater reliability for visual identification (Hussain et al., 2015). Moreover, these visual EEG features have limited predictive value for treatment response (Demarest et al., 2017). These issues contribute to misdiagnoses and delays in achieving seizure remission, which negatively impact patient outcomes (Primec et al., 2006; Riikonen,

2010). Therefore, FCNs, as a supplement to traditional visual EEG analysis, may play an important role in enhancing the effective treatment of spasms, improving seizure control, and maximizing long-term developmental outcomes.

To test this, we retrospectively analyzed scalp EEG data from 21 subjects with infantile spasms (both pre- and post-treatment recordings) and 21 normal, approximately age-matched controls (Shrey et al., 2018). FCNs were calculated using a connectivity measure based on cross-correlation (Chu et al., 2012; Kramer et al., 2009).

5.2 Patients exhibiting epileptic spasms have stronger functional connections.

We first compared FCNs for patients exhibiting spasms (n=31, including pre-treatment IS subjects and post-treatment non-responders) and patients without spasms (n=32, including controls and post-treatment responders). Patients with epileptic spasms had stronger functional connections compared to those without spasms (Figure 6A). A Wilcoxon rank sum test indicated that of the 171 pairs of electrodes, 56 pairs were significantly different between the spasms and non-spasms groups ($p < 0.05$ pre-specified threshold FDR, Benjamini-Hochberg procedure for multiple comparisons correction; pFDR = 0.016; q-value = 0.016). Fifty-five pairs had higher median connectivity strength for patients with spasms, and one pair (Cz-O2) showed the opposite relationship.

5.3 EEG-based FCNs exhibit high test-retest reliability over short periods of time.

We tested the reliability of the FCN calculation by measuring the 2D correlation between independent FCNs generated using sequential, non-overlapping segments of EEG (Figure 6B). FCN measurements for all subjects were stable when calculated using segments of EEG at least ~150 seconds long. However, as a group, the spasms FCNs exhibited higher reliability than those of control subjects.

5.4 While connectivity strength varies with disease state, the patient-specific FCN structure can be stable over long periods of time.

In individual subjects, successful treatment of spasms was associated with a reduction in FCN strength to control levels over several weeks (Shrey et al., 2018). However, the patient-specific structure of the networks (indicated by the spatial pattern of the strongest connections) often persisted, particularly when treatment was unsuccessful. To demonstrate this, we analyzed a longitudinal EEG recording from a spasms patient who later developed Lennox-Gastaut Syndrome. The strength of the FCN increased at the onset of Lennox-Gastaut, but the structure of the network remained stable over 17 months, during which the patient experienced continued seizures despite multiple changes in medication (Figure 6C).

These results demonstrate the potential value of EEG-based FCNs as a marker of infantile spasms and epileptic encephalopathies. Computational metrics, such as FCN strength, are

objective, reliable, and can complement traditional visual analysis. Once validated through larger, prospective studies, EEG-based FCNs may help clinicians diagnose spasms, identify high-risk children, and objectively measure treatment response, leading to earlier resolution of spasms and more favorable outcomes for this vulnerable population.

6.1 Overall Conclusion

Historically, EEG analysis has largely been restricted to subjective visual interpretation. Modern EEG technology is ideal for a new era of data analysis. The examples described in this work demonstrate the current state-of-the-art in applying network analyses to EEG data. These works show the wide range of technologies now available for epilepsy research, as well as their tremendous potential for augmenting standard clinical care and providing predictive guidance to clinicians.

Acknowledgements:

Funding:

This work was supported by the National Institutes of Health [grant numbers: R01NS094399 (to W.S), R01NS095369 (to M.A.K.), R21NS103112 (to S.V.S.), R01NS099348 (to D.B.), NS106957 (to R.S.)]; National Science Foundation [DMS award # 1451384 (to M.A.K.)]; the American Epilepsy Society (S.V.S.); Children's Hospital of Orange County Pediatric Subspecialty Faculty Tithe Grant (to V.L. and B.L.).

References

Adebimpe A, Aarabi A, Bourel-Ponchel E, Mahmoudzadeh M, Wallois F, 2016 EEG Resting State Functional Connectivity Analysis in Children with Benign Epilepsy with Centrotemporal Spikes. Frontiers in neuroscience 10, 143. [PubMed: 27065797]

Bassett DS, Sporns O, 2017 Network neuroscience. Nature neuroscience 20, 353–364. [PubMed: 28230844]

Bassett DS, Zurn P, Gold JI, 2018 On the nature and use of models in network neuroscience. Nat Rev Neurosci 19, 566–578. [PubMed: 30002509]

Bowyer SM, 2016 Coherence a measure of the brain networks: past and present. Neuropsychiatric Electrophysiology 2, 1.

Brazier MA, 1972 Spread of seizure discharges in epilepsy: anatomical and electrophysiological considerations. Exp Neurol 36, 263–272. [PubMed: 4559716]

Bulacio JC, Jehi L, Wong C, Gonzalez-Martinez J, Kotagal P, Nair D, Najm I, Bingaman W, 2012 Long-term seizure outcome after resective surgery in patients evaluated with intracranial electrodes. Epilepsia 53, 1722–1730. [PubMed: 22905787]

Burroughs SA, Morse RP, Mott SH, Holmes GL, 2014 Brain connectivity in West syndrome. Seizure 23, 576–579. [PubMed: 24794162]

Butts CT, 2009 Revisiting the foundations of network analysis Science (New York, N.Y 325, 414–416. [PubMed: 19628855]

Chu CJ, Kramer MA, Pathmanathan J, Bianchi MT, Westover MB, Wizon L, Cash SS, 2012 Emergence of stable functional networks in long-term human electroencephalography. J. Neurosci 32, 2703–2713. [PubMed: 22357854]

Clemens B, Puskas S, Spisak T, Lajtos I, Opposits G, Besenyei M, Hollody K, Fogarasi A, Kovacs NZ, Fekete I, Emri M, 2016 Increased resting-state EEG functional connectivity in benign childhood epilepsy with centro-temporal spikes. Seizure 35, 50–55. [PubMed: 26794010]

Demarest ST, Shellhaas RA, Gaillard WD, Keator C, Nickels KC, Hussain SA, Loddenkemper T, Patel AD, Saneto RP, Wirrell E, Sanchez Fernandez I, Chu CJ, Grinspan Z, Wusthoff CJ, Joshi S, Mohamed IS, Stafstrom CE, Stack CV, Yozawitz E, Bluvstein JS, Singh RK, Knupp KG, 2017 The

impact of hypsarrhythmia on infantile spasms treatment response: Observational cohort study from the National Infantile Spasms Consortium. Epilepsia 58, 2098–2103. [PubMed: 29105055]

Dempster AP, Laird NM, Rubin DB, 1977 Maximum likelihood from incomplete data via the EM algorithm. Journal of the Royal Statistical Society. Series B (Methodological) 39, 1–38.

Feldt Muldoon S, Soltesz I, Cossart R, 2013 Spatially clustered neuronal assemblies comprise the microstructure of synchrony in chronically epileptic networks. Proc Natl Acad Sci U S A 110, 3567–3572. [PubMed: 23401510]

Gonzalez-Martinez JA, Srikijvilaikul T, Nair D, Bingaman WE, 2007 Long-term seizure outcome in reoperation after failure of epilepsy surgery. Neurosurgery 60, 873–880; discussion 873–880. [PubMed: 17460523]

Gotman J, 1983 Measurement of small time differences between EEG channels: method and application to epileptic seizure propagation. Electroencephalography and clinical neurophysiology 56, 501–514. [PubMed: 6194969]

Gramfort A, Luessi M, Larson E, Engemann DA, Strohmeier D, Brodbeck C, Parkkonen L, Hamalainen MS, 2014 MNE software for processing MEG and EEG data. NeuroImage 86, 446–460. [PubMed: 24161808]

Greenblatt RE, Pflieger ME, Ossadtchi AE, 2012 Connectivity measures applied to human brain electrophysiological data. Journal of neuroscience methods 207, 1–16. [PubMed: 22426415]

Gunnarsdottir KM, Bulacio J, Gonzalez-Martinez J, Sarma SV, 2019 Estimating Intracranial EEG Signals at Missing Electrodes in Epileptic Networks, 2019 41st Annual International Conference of the IEEE Engineering in Medicine and Biology Society (EMBC), pp. 3858–3861.

Gunnarsdottir KM, Li A, Bulacio J, Gonzalez-Martinez J, Sarma SV, 2017 Estimating unmeasured invasive EEG signals using a reduced-order observer. Conf Proc IEEE Eng Med Biol Soc 2017, 3216–3219. [PubMed: 29060582]

Horstmann MT, Bialonski S, Noennig N, Mai H, Prusseit J, Wellmer J, Hinrichs H, Lehnertz K, 2010 State dependent properties of epileptic brain networks: comparative graph-theoretical analyses of simultaneously recorded EEG and MEG. Clin. Neurophysiol 121, 172–185. [PubMed: 20045375]

Hrachovy RA, Frost JD Jr., 2003 Infantile epileptic encephalopathy with hypsarrhythmia (infantile spasms/West syndrome). J. Clin. Neurophysiol 20, 408–425. [PubMed: 14734931]

Hrachovy RA, Frost JD Jr., Kellaway P, 1984 Hypsarrhythmia: variations on the theme. Epilepsia 25, 317–325. [PubMed: 6539199]

Hussain SA, Kwong G, Millichap JJ, Mytinger JR, Ryan N, Matsumoto JH, Wu JY, Lerner JT, Sankar R, 2015 Hypsarrhythmia assessment exhibits poor interrater reliability: a threat to clinical trial validity. Epilepsia 56, 77–81. [PubMed: 25385396]

Japaridze N, Muthuraman M, Moeller F, Boor R, Anwar AR, Deuschl G, Stephani U, Raethjen J, Siniatchkin M, 2013 Neuronal networks in west syndrome as revealed by source analysis and renormalized partial directed coherence. Brain Topogr. 26, 157–170. [PubMed: 23011408]

Jiruska P, de Curtis M, Jefferys JG, Schevon CA, Schiff SJ, Schindler K, 2013 Synchronization and desynchronization in epilepsy: controversies and hypotheses. The Journal of physiology 591, 787–797. [PubMed: 23184516]

Karlis D, Xekalaki E, 2003 Choosing initial values for the EM algorithm for finite mixtures. Comput Stat Data An 41, 577–590.

Khambhati AN, Bassett DS, Oommen BS, Chen SH, Lucas TH, Davis KA, Litt B, 2017 Recurring Functional Interactions Predict Network Architecture of Interictal and Ictal States in Neocortical Epilepsy. eNeuro 4.

Khambhati AN, Kahn AE, Costantini J, Ezzyat Y, Solomon EA, Gross RE, Jobst BC, Sheth SA, Zaghloul KA, Worrell G, Seger S, Lega BC, Weiss S, Sperling MR, Gorniak R, Das SR, Stein JM, Rizzuto DS, Kahana MJ, Lucas TH, Davis KA, Tracy JI, Bassett DS, 2019 Functional control of electrophysiological network architecture using direct neurostimulation in humans. Netw Neurosci 3, 848–877. [PubMed: 31410383]

Kramer M, Eden U, Cash S, Kolaczyk E, 2009 Network inference with confidence from multivariate time series. Physical Review E 79.

Lachaux JP, Rodriguez E, Martinerie J, Varela FJ, 1999 Measuring phase synchrony in brain signals. Hum Brain Mapp 8, 194–208. [PubMed: 10619414]

Li A, Gunnarsdottir KM, Inati S, Zaghloul K, Gale J, Bulacio J, Martinez-Gonzalez J, Sarma SV, 2017 Linear time-varying model characterizes invasive EEG signals generated from complex epileptic networks. Conf Proc IEEE Eng Med Biol Soc 2017, 2802–2805. [PubMed: 29060480]

Litt B, Esteller R, Echauz J, D'Alessandro M, Shor R, Henry T, Pennell P, Epstein C, Bakay R, Dichter M, Vachtsevanos G, 2001 Epileptic seizures may begin hours in advance of clinical onset: a report of five patients. Neuron 30, 51–64. [PubMed: 11343644]

Luders HO, Najm I, Nair D, Widdess-Walsh P, Bingman W, 2006 The epileptogenic zone: general principles. Epileptic Disord 8 Suppl 2, S1–9.

Luenberger DG, 1964 Observing the state of a linear system. IEEE Trans Mil Electr 8, 74–80.

Mori S, Wu D, Ceritoglu C, Li Y, Kolasny A, Vaillant MA, Faria AV, Oishi K, Miller MI, 2016 MRICloud: Delivering High-Throughput MRI Neuroinformatics as Cloud-Based Software as a Service. Comput Sci Eng 18, 21–35.

Pasqualetti F, Zampieri S, Bullo F, 2014 Controllability Metrics, Limitations and Algorithms for Complex Networks. 2014 American Control Conference (Acc), 3287–3292.

Pereda E, Quiroga RQ, Bhattacharya J, 2005 Nonlinear multivariate analysis of neurophysiological signals. Prog Neurobiol 77, 1–37. [PubMed: 16289760]

Primec ZR, Stare J, Neubauer D, 2006 The risk of lower mental outcome in infantile spasms increases after three weeks of hypsarrhythmia duration. Epilepsia 47, 2202–2205. [PubMed: 17201726]

Quraan MA, McCormick C, Cohn M, Valiante TA, McAndrews MP, 2013 Altered resting state brain dynamics in temporal lobe epilepsy can be observed in spectral power, functional connectivity and graph theory metrics. PloS one 8, e68609. [PubMed: 23922658]

Riikonen RS, 2010 Favourable prognostic factors with infantile spasms. Eur J Paediatr Neurol 14, 13–18. [PubMed: 19362867]

Rubinov M, Sporns O, 2010 Complex network measures of brain connectivity: uses and interpretations. NeuroImage 52, 1059–1069. [PubMed: 19819337]

Shipton HW, 1975 EEG analysis: a history and a prospectus. Annu Rev Biophys Bioeng 4, 1–13. [PubMed: 1098549]

Shrey DW, Kim McManus O, Rajaraman R, Ombao H, Hussain SA, Lopour BA, 2018 Strength and stability of EEG functional connectivity predict treatment response in infants with epileptic spasms. Clin. Neurophysiol 129, 2137–2148. [PubMed: 30114662]

Siniatchkin M, van Baalen A, Jacobs J, Moeller F, Moehring J, Boor R, Wolff S, Jansen O, Stephani U, 2007 Different neuronal networks are associated with spikes and slow activity in hypsarrhythmia. Epilepsia 48, 2312–2321. [PubMed: 17645543]

Soares JM, Marques P, Alves V, Sousa N, 2013 A hitchhiker's guide to diffusion tensor imaging. Front Neurosci 7, 31. [PubMed: 23486659]

Spencer E, Martinet LE, Eskandar EN, Chu CJ, Kolaczyk ED, Cash SS, Eden UT, Kramer MA, 2018 A procedure to increase the power of Granger-causal analysis through temporal smoothing. Journal of neuroscience methods 308, 48–61. [PubMed: 30031776]

Stacey WC, Litt B, 2008 Technology insight: neuroengineering and epilepsy-designing devices for seizure control. Nature clinical practice 4, 190–201.

Stefan H, Lopes da Silva FH, 2013 Epileptic neuronal networks: methods of identification and clinical relevance. Front Neurol 4, 8. [PubMed: 23532203]

van Diessen E, Diederen SJ, Braun KP, Jansen FE, Stam CJ, 2013 Functional and structural brain networks in epilepsy: what have we learned? Epilepsia 54, 1855–1865. [PubMed: 24032627]

Warren CP, Hu S, Stead M, Brinkmann BH, Bower MR, Worrell GA, 2010 Synchrony in normal and focal epileptic brain: the seizure onset zone is functionally disconnected. Journal of neurophysiology 104, 3530–3539. [PubMed: 20926610]

Yao D, 2001 A method to standardize a reference of scalp EEG recordings to a point at infinity. Physiol Meas 22, 693–711. [PubMed: 11761077]

Highlights:

- Network analysis and functional connectivity provide unique insights into seizure networks
- Observers from control theory can be used to estimate missing intracranial EEG signals to provide denser brain coverage
- Graph theory predicts that stimulation has predictable and variable effects on different network structures
- Functional connectivity can be used to assess the response to antiepileptic therapy in infantile spasms

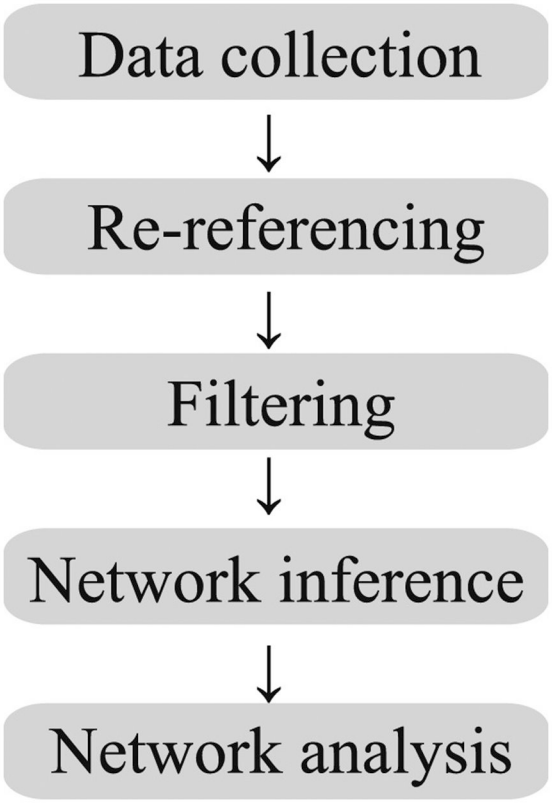

Figure 1: A candidate functional network analysis pipeline, with five steps.
While the arrows indicate a linear progression between steps, the interactions between steps are more complicated.

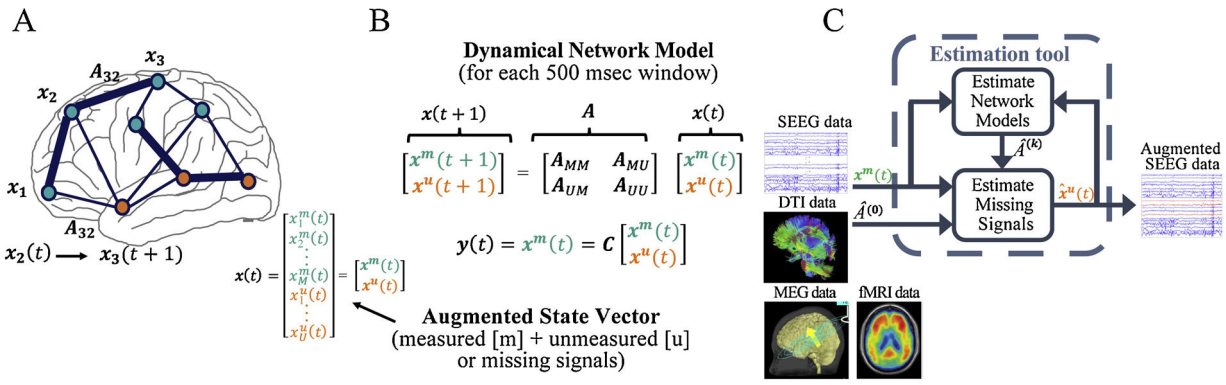

Figure 2: Network model set-up

A) Definition of model states. B) Network model for each 500 msec window of EEG. C) Flowchart of the computational tool. Structural (e.g. DTI) and functional (e.g. SEEG) information are inputs to the algorithm, which produces an augmented denser coverage.

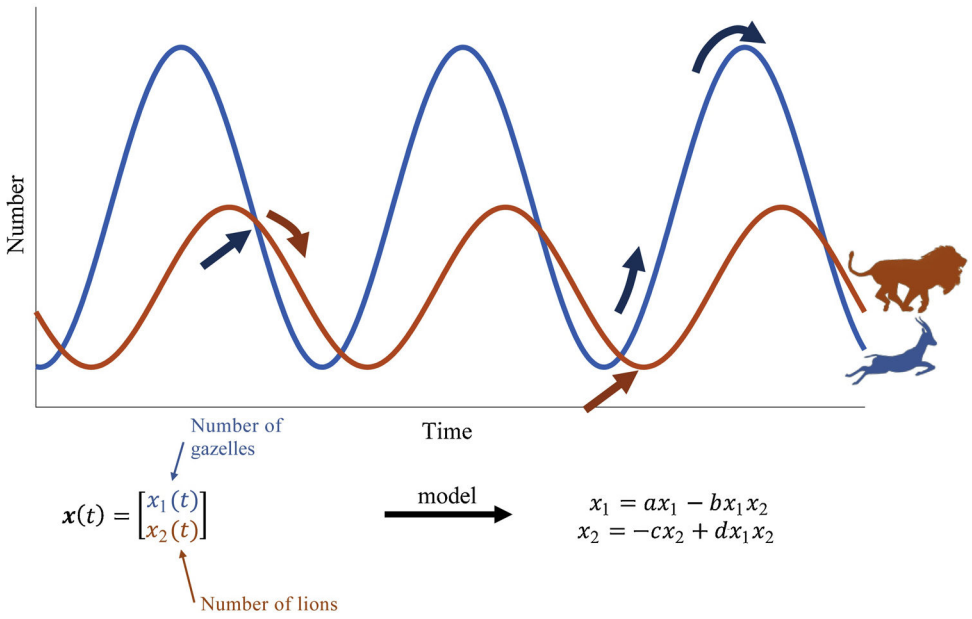

Figure 3: Predator-prey model

(Top) Population of lions and gazelles over time. (Bottom) Dynamical 2-node network model describing populations over time, assigning a differential equation for each population.

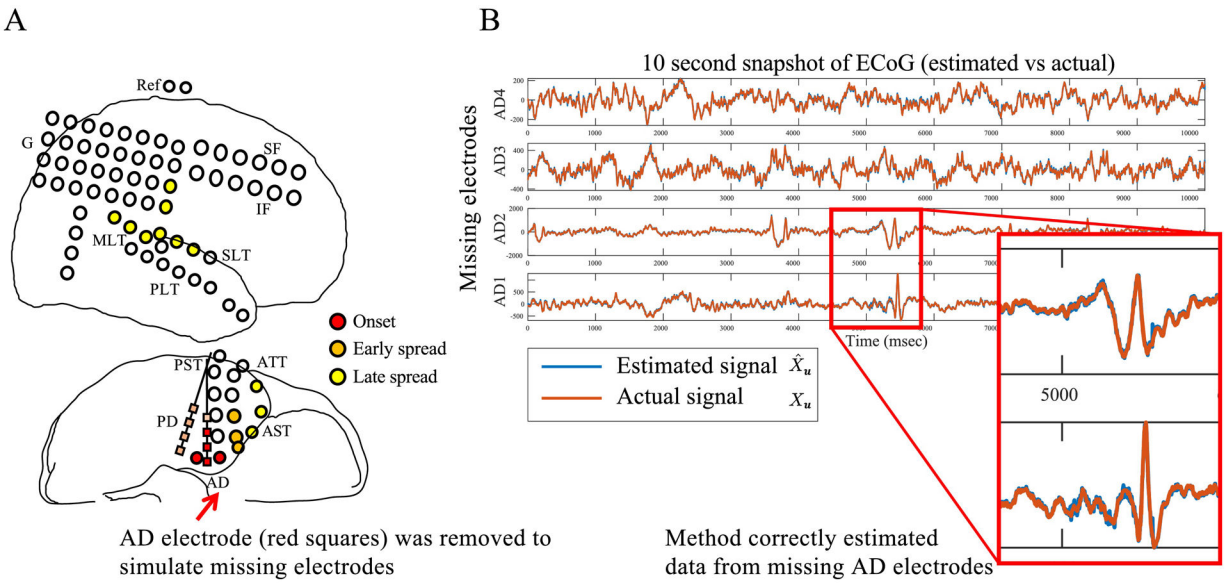

Figure 4: Estimating signals of missing electrodes

A) ECoG implantation for patient. B) 10 second snapshot of actual (red) versus estimated (blue) signals of 4 missing contacts from one depth electrode. Two contacts were clinically labeled as early onset zone because of spikes highlighted in zoom-in panel shown. Note that no spikes were visible in all other signals, demonstrating that with knowledge of network model, the observer is able to very accurately reconstruct missing contact signals, including important spike events.

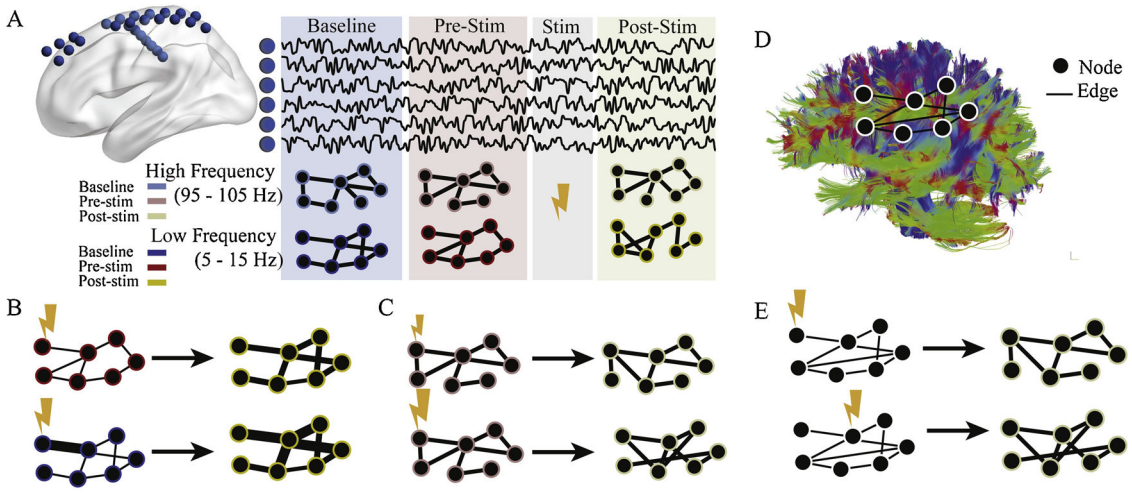

Figure 5: Graph theory to estimate different responses to electrical stimulation

(A) Methods and experimental design. 94 individuals with implanted intracranial EEG electrodes (blue spheres) voluntarily participated in a stimulation regimen. Each subject had baseline (blue) recording with no stimulation, followed by several stimulation trials, with pre- (red) and post-stimulation (yellow) epochs. For each of these epochs, functional networks were constructed by calculating multi-taper coherence between all electrodes in one of four frequency bands (5–15 Hz, 15–25 Hz, 30–40Hz, or 95–105 Hz). Only two are shown for simplicity. (B, top) In low frequencies (5–15 Hz), the node strengths, or sum of connection weights, increase between pre- and post-stimulation epochs. (B, bottom) Nodes with high baseline coherence to the stimulated region have larger increases in strength. (C) In high frequencies (95–105 Hz), the pattern of edge similarity changes with stimulation. This change is larger for stimulation with higher frequency (bottom). (D) An example of a structural brain network obtained with DWI, where edges are proportional to the density of white matter connections between regions. (E) When stimulating structural nodes that are weakly connected (top), functional connectivity patterns of the high frequency band undergo less reorganization than when stimulating structural nodes that are strongly connected (bottom).

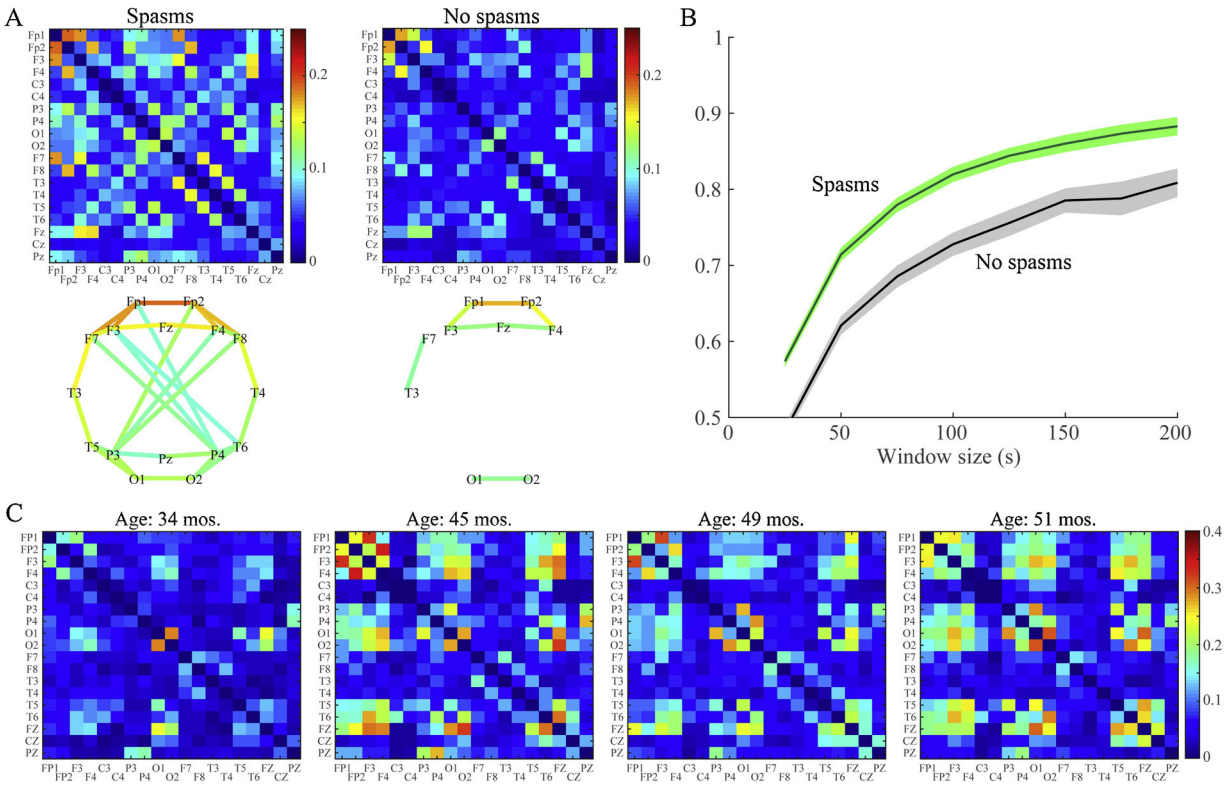

Figure 6: Epileptic spasms are associated with strong, stable functional networks.

(A) Average functional connectivity matrices (top row) and network maps (bottom row) for patients with and without spasms. The color represents the connectivity strength, defined as the proportion of 1-second epochs for which the connectivity between two channels was statistically significant. Network maps show all connections with strength > 0.1. (B) Test-retest reliability of the FCN for the spasms group (green) and the non-spasms group (gray) measured via 2D correlation of the connectivity matrices for EEG segments of varying length. The solid lines represent the mean, and shaded areas denote the 95% confidence interval across all subjects in the group. FCNs are reliable when measured using segments of EEG at least 150 seconds long, and the spasms group exhibited higher reliability than controls. (C) A representative example of FCNs from longitudinal EEGs of a patient who had spasms and was diagnosed with Lennox-Gastaut at 45 months old. The strength of the FCN increases with onset of Lennox-Gastaut and varies over time; however, note that the locations of the strongest connections in the network remain stable over the 17 month period. This patient experienced continued seizures, despite multiple medication changes.